

# Estimated Visual Magnitudes of the EISCAT UHF Meteors

Csilla Szasz · Johan Kero · Asta Pellinen-Wannberg · David D. Meisel · Gudmund Wannberg · Assar Westman

Received: 30 June 2007 / Accepted: 29 November 2007 / Published online: 18 December 2007  
© Springer Science+Business Media B.V. 2007

**Abstract** We have investigated the conditions for simultaneous meteor observations with the EISCAT UHF radar system and telescopic optical devices. The observed characteristics of 410 meteors detected by all three UHF receivers are compared with model simulations and their luminosity is calculated as a part of a meteoroid ablation model using a fifth order Runge–Kutta numerical integration technique. The estimated absolute visual magnitudes are in the range of +9 to +5. The meteors should therefore be observable using intensified CCD or EMCCD (Electron Multiplying CCD) cameras with telephoto lenses. A possible setup of a coordinated radar and optical campaign is suggested.

**Keywords** Meteor · EISCAT · HPLA · Radar · Magnitude · Optical detection

## Abbreviations

EISCAT European incoherent scatter facility  
HPLA High power large aperture  
EMCCD Electron multiplying CCD

## 1 Introduction

Simultaneous high-resolution optical and radar observations of meteors are of great importance in the further understanding of the meteoroid-atmosphere interaction processes

---

C. Szasz (✉) · J. Kero  
Swedish Institute of Space Physics, Kiruna, Sweden  
e-mail: csilla@irf.se

A. Pellinen-Wannberg  
Umeå University and Swedish Institute of Space Physics, Kiruna, Sweden

D. D. Meisel  
SUNY Geneseo, Geneseo, NY, USA

G. Wannberg · A. Westman  
EISCAT Scientific Association, Kiruna, Sweden

and the physics of the head echo. The head echoes observed with the meteor radar at the Springhill Meteor Observatory all had visual magnitudes in the range of +4 to -4 when detected optically (Jones and Webster 1991). Similar radar head echo and optical observations at High Power Large Aperture (HPLA) radar facilities have with one exception hitherto not succeeded due to the low light emission levels of typical HPLA meteors and problems with interference between transmitter equipment and collocated optical devices. One attempt is presented in Pellinen-Wannberg et al. (1998). Nishimura et al. (2001) have with the MU (Middle and Upper atmosphere) 46.5 MHz radar and one camera successfully recorded meteors down to magnitudes of +9.

The purpose of this study is to investigate the requisites and suitable conditions for simultaneous meteor observations with telescopic optical devices and the EISCAT UHF radar system. The radar operating frequency around 930 MHz and its three separate receivers at 200–400 km distance from each other would together with two optical devices provide excellent opportunities to compare the head echo scattering characteristics in the UHF band with optical emissions and investigate the accuracy of the two independent velocity and trajectory determination methods.

A short review of the EISCAT UHF system and the most recent meteor campaigns is given in Sect. 2. In Sects. 3 and 4 we present the procedure of estimating the visual magnitudes of the observed radar meteors by fitting their measured deceleration to a single object, numerical ablation model. Meteoroid ablation was described already by Öpik (1958) and further developed by Bronshten (1983) and Love and Brownlee (1991). We have in our calculations been guided by Rogers et al. (2005) who have combined the works mentioned and also added a sputtering model adopted from Tielens et al. (1994). We conclude that the absolute visual magnitudes of the EISCAT UHF meteors are in the range of +9 to +5 and present a possible setup of a coordinated radar and optical campaign in Sect. 5.

## 2 EISCAT UHF Observations

Four dedicated meteor experiments were run on the EISCAT UHF system between 2002 and 2005, as summarized in Table 1. Data was collected at vernal/autumnal equinox and summer/winter solstice.

The EISCAT 930 MHz UHF radar system comprises three 32 m paraboloïds. A transmitter/receiver is located near Tromsø Norway, at 69.6° N, 19.2° E and two remote receivers are sited in Kiruna, Sweden, at 67.9° N, 20.4° E and Sodankylä, Finland, at 67.4° N, 26.6° E. All three antennae were pointed towards a common volume at a height of 96 km, the peak of the EISCAT UHF altitude distribution of detected meteors (Westman et al. 2004). The position of the common volume was 68.9° N and 21.9° E. The configuration used is of tetrahedron geometry as drawn in Fig. 1.

**Table 1** Dates and times for meteor campaigns with the EISCAT UHF system

	Year	Start (UT)	Stop (UT)	No of events
Vernal equinox	2002	Mar 19, 12:00	Mar 20, 12:00	50
Summer solstice	2005	Jun 21, 14:00	Jun 22, 10:00	101
	2005	Jun 23, 10:00	Jun 23, 14:00	
Autumnal equinox	2005	Sep 21, 07:00	Sep 22, 07:00	194
Winter solstice	2004	Dec 21, 08:00	Dec 22, 08:00	65

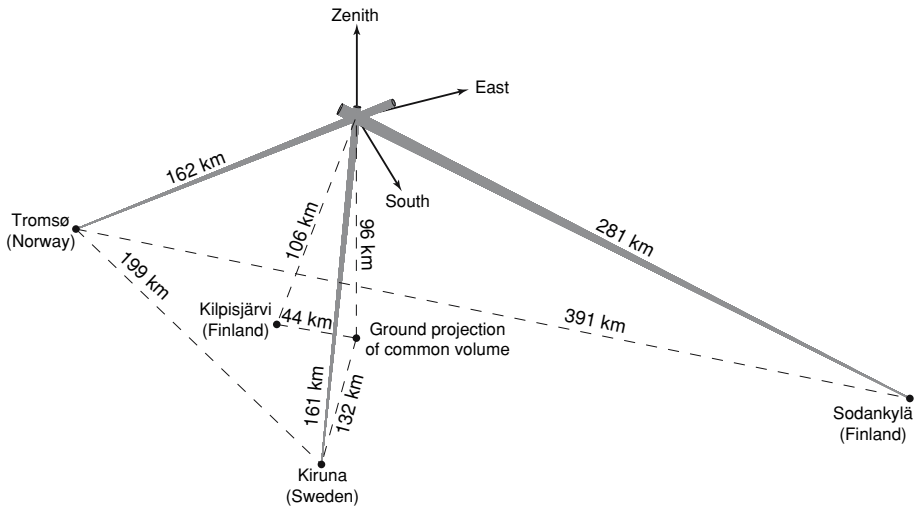


**Fig. 1** Meteor observing geometry of the EISCAT UHF system with ranges from the transmitter/receiver and the two remote receivers to the common volume as well as ground distances between the sites. Distances are also indicated from Kiruna and Kilpisjärvi to the ground projection of the common volume

For meteoroids detected by all three receivers simultaneously, the precise geocentric velocity can be calculated. The velocity components measured by the remote receivers are pointing in the directions of the bisectors, defined in the plane spanned by each remote receiver's line-of-sight and the transmitter's line-of-sight. By dividing each velocity component along the bisectors and the Tromsø line-of-sight into orthogonal  $x$ ,  $y$  and  $z$  components, three equations (one for each site) are obtained, with three unknowns (the three components of the velocity vector). The geocentric speed as a function of time (or position) of each meteoroid is then simply found by calculating the norm of the velocity vector for each interpulse period.

The results presented here are based on 410 tristatic meteor events which contain enough data points for line-of-sight velocity calculation to be compared to the Doppler velocity measurements.

### 3 Ablation Model

We have implemented a single-object ablation model to compare our observations with. The model is similar to Rogers et al. (2005) and references therein, originally based on Öpik (1958), Bronshten (1983) and Love and Brownlee (1991) with a sputtering model added described by Tielens et al. (1994). The input meteoroid parameters to the model are above-atmosphere velocity, mass, density and zenith distance. MSIS-E-90 (Hedin 1991) is used for atmospheric densities.

The radar cross section is estimated by assuming overdense scattering in the Rayleigh regime, and calculated in a similar fashion as described in Westman et al. (2004) and Close et al. (2002). Due to the hypersonic flow, we let the meteoric atoms constituting the mass loss in the ablation model expand radially outwards with a compressed mean free path adopted from Bronshten (1983). We assume that the head echo originates from an overdense region in the immediate vicinity of the meteoroid and use the primary ionization

**Table 2** Values of parameters used in the ablation model

Parameter	Value	Unit
Meteoroid shape factor (spherical)	$\frac{\pi}{(4\pi/3)^{2/3}} \simeq 1.21$	
Specific heat of meteoroid	1200	J/K/kg
Clausius-Clapeyron coefficients	10.6, 13500–16120 K	
Emissivity	0.9	
Drag coefficient	1	
Heat transfer coefficient	0.2, 0.4, 0.6, 0.8, 1.0	
Latent heat of fusion + vaporization	$6.0 \cdot 10^6$	J/kg
Mean molecular mass of ablated vapour	56, 50, 20, 20	u
Meteoroid density	7800, 3300, 1000, 300	kg/m <sup>3</sup>
Effective atmospheric temperature	280	K

coefficient of Jones (1997) and a spherical, collisionless expansion of the produced electrons to calculate the electron density. The size of the modelled Rayleigh target corresponds to the radial distance from the meteoroid at which the electron density equals the critical density of the UHF wave, about  $10^{16}/\text{m}^3$ .

We have compared and fitted the precise particle deceleration and radar cross section obtained from the tristatic data to the ablation model by adjusting the input parameters propagated down through the atmosphere to our observation altitude using a fifth order Runge–Kutta numerical integration technique with a variable step size (Danby 1988). Four different densities, 0.3 g/cc for porous, 1 g/cc for cometary, 3.3 g/cc for asteroidal and 7.8 g/cc for iron material, were paired with mean molecular mass of ablated vapour of 20 u for graphite (both porous and cometary material), 50 u for silicon dioxide and 56 u for iron respectively (Tielens et al. 1994; Rogers et al. 2005). Every pair of density and molecular mass was propagated down through the atmosphere using every one of five different heat transfer coefficients, 0.2, 0.4, 0.6, 0.8 and 1. Each combination was fitted to the data by iteratively adjusting the input parameters and minimizing the least-square difference between model and measurements. Then the best of the fits was chosen and its input values used as estimates for the extra-atmospheric properties of our observed meteoroids. Other model parameters used are further described in Table 2.

The mass distribution found by this method is very similar to the one reported for the ALTAIR radar by Close et al. (2007).

#### 4 Luminosity and Magnitude

Emitted power  $I$  [W] of each meteor is estimated as

$$I = \tau(v) \cdot \frac{dm}{dt} \cdot \frac{v^2}{2} \quad (1)$$

with the luminous efficiency  $\tau(v)$  suggested by Hill et al. (2005). The mass loss due to ablation and sputtering,  $\frac{dm}{dt}$ , is estimated with the ablation model and  $v^2$  is the measured

meteoroid velocity. The maximum illuminance  $I_V$  [lux] in the visual band at a distance of  $R = 100$  km is calculated as

$$I_V = \frac{683}{4\pi \cdot R^2} \cdot I. \tag{2}$$

The maximum absolute magnitude  $M_V$  in the visual band

$$M_V = -2.5 \cdot \log I_V - 14.2 \tag{3}$$

is plotted as a function of above-atmosphere meteoroid mass in Fig. 2a. Apparent magnitude  $m_V$  at the Kiruna receiver station ( $R_{kir} = 161$  km)

$$m_V = M_V + 5 \cdot (\log R_{kir} - 5) \tag{4}$$

is plotted as a function of above-atmosphere meteoroid velocity in Fig. 2b. The equations above can be found in almost any elementary textbook in astrophysics. The estimated absolute visual magnitudes are in the range of +9 to +5.

If a meteoroid has broken up into pieces before or during the observation, the measured deceleration represents the biggest remaining fragment (Ceplecha et al. 1998). The calculated luminosity is in this case an underestimation as the modelled ablation applies to this particular fragment only and not the sum of all fragments.

The uncertainties of the derived parameters introduced by errors in the measured radar cross-section and deceleration are small compared to the uncertainties introduced by the model assumptions. If we for example select a different meteoroid density than that determined as the most suitable one, the value of the above-atmospheric mass for a particular meteoroid may differ by an order of magnitude. The absolute visual magnitude generally changes with a value of less than one and the atmospheric entry velocity changes with a few percent.

Model assumptions as well as the role of fragmentation may be resolved by simultaneous optical and radar measurements. The accuracy of the present study is high enough for a feasibility study.

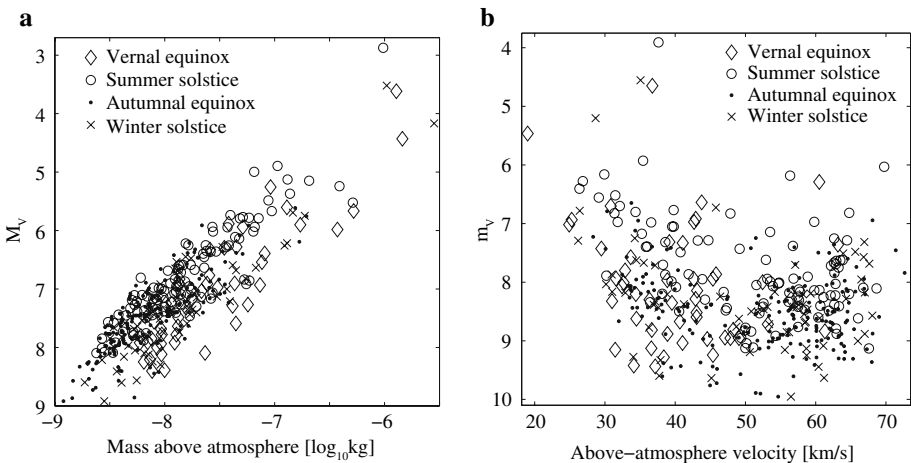


**Fig. 2** (a) Absolute magnitude versus mass and (b) apparent magnitude as seen from the Kiruna site versus velocity

## 5 Conclusions and Future Work

The estimated visual magnitudes presented in this paper are comparable with the statistical estimations made by Pellinen-Wannberg et al. (1998) on a previous set of EISCAT meteor observations. According to both studies, the meteors should be observable using an intensified CCD or EMCCD camera with a telephoto lens.

The risk of interference from the high-power transmitter equipment makes the Tromsø site an inappropriate camera location. We propose to use two cameras, one collocated with the Kiruna receiver to enable direct comparisons between radar and optical observations, and a second one located in Kilpisjärvi, Finland, at 69.0° N and 20.9° E. A camera in Kilpisjärvi would provide a good complement to observations made in Kiruna. The elevation angle to the common volume is 65° and the azimuth makes an almost right angle with the Kiruna site azimuth (see Fig. 1).

As reported in Table 1, the highest meteor detection rates are found in autumn, when the apex source is circumpolar. The higher count rates are according to Fig. 2a–b caused by an excessive amount of faint meteors as compared to other seasons. As these faint meteors are most numerous in HPLA measurements, the optical equipment should be selected with an aim of observing them. The brightest meteors seem to be detected in summer, but the EISCAT UHF system being located above the Arctic Circle make optical observations from late spring to early autumn impossible. In late autumn, the night sky is dark enough for optical measurements and the outdoor temperature is tolerable for equipment and observers compared to winter conditions. Another factor to take into account is the geomagnetic activity as auroral emissions may outshine faint meteors. In summary, a coordinated measuring campaign as suggested in this study should be scheduled around or after autumnal equinox, in a period when the moon is close to new.

**Acknowledgements** We gratefully acknowledge the EISCAT staff for their assistance during the experiment. EISCAT is an international association supported by research organisations in China (CRIPR), Finland (SA), France (CNRS), Germany (DFG), Japan (NIPR and STEL), Norway (NFR), Sweden (VR) and the United Kingdom (STFC). Two of the authors (CS and JK) are financed by the Swedish National Graduate School of Space Technology.

## References

- V.A. Bronshten, *Physics of Meteoric Phenomena*. (D. Reidel Publishing Company, 1983)
- Z. Ceplecha, J. Borovička, W.G. Elford, D.O. Revelle, R.L. Hawkes, V. Porubčan, M. Šimek, *Space Sci. Rev.* **84**, 327–471 (1998)
- S. Close, M. Oppenheim, S. Hunt, L. Dyrud, *J. Geophys. Res. (Space Phys.)* **107**, 9–1 (2002)
- S. Close, P. Brown, M. Campbell-Brown, M. Oppenheim, P. Colestock, *Icarus* **186**, 547–556 (2007)
- J.M.A. Danby, *Fundamentals of celestial mechanics*, 2nd. rev. and enlarged edn. (Willmann-Bell, 1988)
- A.E. Hedin, *J. Geophys. Res.* **96**, 1159–1172 (1991)
- K.A. Hill, L.A. Rogers, R.L. Hawkes, *Astron. Astrophys.* **444**, 615–624 (2005)
- W. Jones, *Mon. Not. R. Astron. Soc.* **288**, 995–1003 (1997)
- J. Jones, A.R. Webster, *Planet. Space Sci.* **39**, 873–878 (1991)
- S.G. Love, D.E. Brownlee, *Icarus* **89**, 26–43 (1991)
- K. Nishimura, T. Sato, T. Nakamura, M. Ueda, *IEICE Trans. Commun.* **E84-C**(12), 1877–1884 (2001)
- E.J. Öpik, *Physics of meteor flight in the atmosphere, No. 6 in Interscience tracts on physics and astronomy* (Interscience Publishers, Inc., 1958)
- A. Pellinen-Wannberg, A. Westman, G. Wannberg, K. Kaila, *Annales Geophysicae* **16**, 1475–1485 (1998)
- L.A. Rogers, K.A. Hill, R.L. Hawkes, *Planet. Space Sci.* **53**, 1341–1354 (2005)
- A.G.G.M. Tielens, C.F. McKee, C.G. Seab, D.J. Hollenbach, *Astrophys. J.* **431**, 321–340 (1994)
- A. Westman, G. Wannberg, A. Pellinen-Wannberg, *Annales Geophysicae* **22**, 1575–1584 (2004)